Journal of Luminescence 298 (2026) 122080

Contents lists available at ScienceDirect

Journal of Luminescence

journal homepage: www.elsevier.com/locate/jlumin

Full Length Article

Comparison of experimental and computational $Bi^{4+/3+}$ charge transition level energies relative to the vacuum level

Pieter Dorenbos

Delft University of Technology, Faculty of Applied Sciences, Department of Radiation Science and Technology, Mekelweg 15, 2629 JB Delft, Netherlands

ARTICLE INFO

Keywords:
Bismuth
Charge transition levels
Valence stability
Charge carrier trapping
Luminescence

ABSTRACT

Bismuth, in the form of Bi^{2+}, Bi^{3+}, and Bi^{4+}, is utilized in luminescence phosphors, scintillators, afterglow phosphors, and storage phosphors. The preferred valence of bismuth, wavelength of emission, quantum efficiency, thermal quenching, and whether bismuth can trap an electron or a hole depend on the location of the $Bi^{3+/2+}$ and $Bi^{4+/3+}$ charge transition levels in the band gap of the inorganic compound. The $Bi^{4+/3+}$ charge transition level energy relative to the vacuum level is equivalent to the vacuum referred binding energy (VRBE) in the ground state of Bi^{3+}. Methods for obtaining Bi^{3+} VRBEs in inorganic compounds have become available past ten years. One method uses experimental data on Bi spectroscopy combined with the semi-empirical chemical shift method that was originally developed for the lanthanides. Another method is fully computational. The $Bi^{4+/3+}$ CTL location above the valence band (VB) top is first computed. A separate computation with the slab and vacuum method provides the energy at the VB-top relative to the vacuum level. Here we will compare the results of both methods to explore to what extend they are consistent with each other.

1. Introduction

The location of the bismuth charge transition levels (CTLs) with respect to the host valence or conduction band controls many fascinating properties of bismuth activated materials. Like for lanthanides, it determines the preferred valence state (Bi^{2+}, Bi^{3+}, Bi^{4+}), it determines whether bismuth is a potential hole trapping or electron trapping center, and also how deep those charge carrier traps are. Luminescence quantum efficiency and thermal quenching temperature have always been difficult to fully understand. Like for the lanthanides it is often linked to electron transfer to the conduction band (CB) or hole transfer to the valence band (VB) and again CTL locations are crucial [1].

Fig. 1 shows the ground and excited states of Bi^{3+} and of Bi^{2+}. Bi^{3+} has $6s^2$ ground state electron configuration and the excited levels belong to the 6s6p electron configuration. The combination of spin-orbit interaction and the interaction with the crystal field provides the characteristic energy level diagram as in Fig. 1(a). For theory on the level energies of $6s^2$ ions, we refer to the review by Ranfagni et al. [2]. Luminescence from the $^3P_1$ to $^1S_0$ level results in ultraviolet or blue emission; the so-called A-band emission. Many studies have been devoted to elucidating the relationship between the A-band energy and the type of host compound. Wang et al. [3] in 2012 use the dielectric theory of the chemical bond to derive an environmental parameter h_e that characterizes the compound. It shows a clear correlation with the observed A-band, and also C-band energy. The same idea was followed by Amer and Boutinaud [4] in 2017. Awater and Dorenbos [5] in 2017 related the A-band energy to the U-parameter, which can be estimated from the electronegativities of the atoms in the compound [6]. Since dielectric bond theory is also related to electronegativity, it is not surprising that the h_e and U are strongly related environmental parameters [7]. Both parameters quantify the so-called nephelauxetic effect. The effect increases with a smaller electronegativity of the anions in the compound (F, Cl, O, Br, S, I, Se). Within the oxides, it tends to increase with a decreasing electronegativity of the cation (P, B, Si, and Al) from phosphates, borates, silicates, to aluminates.

One of the first reviews on Bi luminescence was by Kröger in 1949 [8]. Most phosphate and sulfate compounds of that work reveal UV and blue emissions. These are characteristic for the A-band emission of Bi^{3+}. In some compounds, red emission was observed, and the origin remained open at that time. In the 1968 review by Blasse and Bril [9] on the Bi^{3+} emission in compounds with large trivalent cations, only UV-blue A-band emissions are observed. The red emissions in the compounds of Kröger were later assigned to the emission from Bi^{2+} [10–12]. Fig. 1b shows the ground and excited states of Bi^{2+} that belong to the $6s^26p$ electron configuration. The red emission comes from the $^2P_{3/2}(1)$ excited state.

Around 1970, in the early career of Georges Boulon, the Bi^{3+} doped rare earth (La, Y, Sc) sesquioxides and rare earth orthovanadates were studied [13]. Many papers on Bi^{3+} luminescence have appeared since then [14], and today bismuth is actively studied for different

E-mail address: p.dorenbos@tudelft.nl

https://doi.org/10.1016/j.jlumin.2026.122080
Received 2 February 2026; Accepted 6 July 2026
Available online 22 July 2026

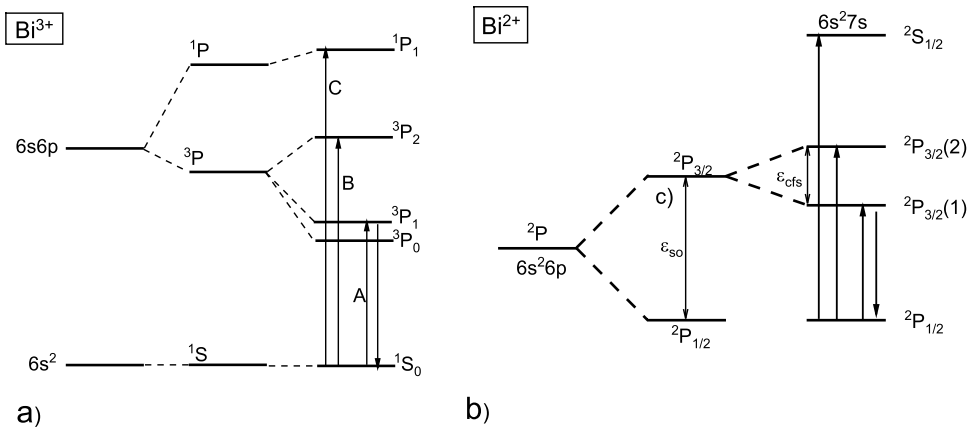

Fig. 1. a) the energy level scheme of Bi^{3+} showing the origin of the $^3P_1 \rightarrow {}^1S_0$ UV-blue A-band emission. b) the energy level scheme of Bi^{2+} showing the origin of the $^2P_{3/2}(1) \rightarrow {}^2P_{1/2}$ red emission.

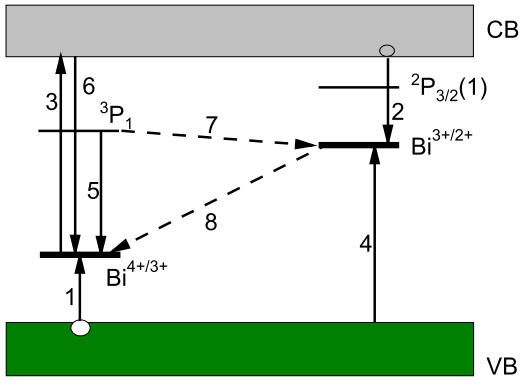

Fig. 2. Scheme showing the $Bi^{4+/3+}$ and $Bi^{3+/2+}$ charge transition levels in the bandgap of a compound. The arrows illustrate the possible charge carrier transfer routes between Bi and the host bands, as well as between Bi-Bi pairs.

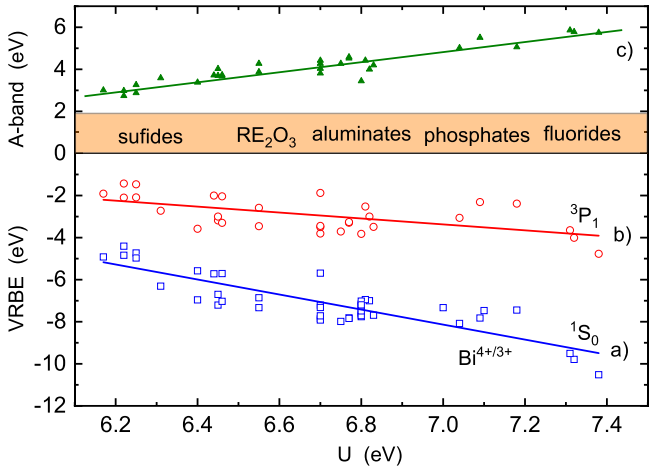

Fig. 3. Data along line a) are the $Bi^{4+/3+}$ CTL energies in Bi-doped compounds relative to the vacuum level against the value for U of that compound as was presented in [5]. It is equivalent to the vacuum referred binding energy in the $^1S_0$ ground state of Bi^{3+}. The VRBE in the $^3P_1$ excited state is shown along line b). Data along line c) are the A-band energy in excitation, i.e., the energy difference between $^3P_1$ and $^1S_0$.

applications. A review on bismuth-activated persistent phosphors can be found in Tang et al. [15]. A review on pure Bi-compounds for photocatalytic hydrogen production was provided by Fang et al. [16] and Meng et al. [17]. Electron transfer from Bi^{3+} to the conduction band or from Bi^{3+} to a neighboring Bi^{3+} gives rise to metal-to-metal charge transfer (MMCT) or Bi-pair emission. Boutinaud provided detailed reviews on those interesting phenomena [18,19].

Whenever charge-carrier transfer from or to Bi^{3+} occurs, the energies of charge transition levels relative to the host valence and conduction band are crucial for understanding the processes involved. This is illustrated in Fig. 2 where the $Bi^{4+/3+}$ and $Bi^{3+/2+}$ CTLs are shown in the bandgap of an example compound. The $Bi^{4+/3+}$ CTL energy is equivalent to the host or vacuum referred electron binding energy (HRBE or VRBE) in the ground state of Bi^{3+}. Likewise, the $Bi^{3+/2+}$ CTL is equivalent to the HRBE or VRBE in the ground state of Bi^{2+}. When the $Bi^{4+/3+}$ CTL is located above the valence band top, as in Fig. 2, Bi^{3+} may trap a valence band hole to form Bi^{4+} (see arrow 1). Similarly when $Bi^{3+/2+}$ is below the conduction band bottom, Bi^{3+} may trap an electron to become Bi^{2+} (see arrow 2). Therefore, in the situation of Fig. 2, Bi^{3+} can trap a hole from the VB but also an electron from the CB. This provides Bi^{3+} doped compounds with charge carrier storage properties. Daylight excites electrons across the bandgap, or from Bi^{3+} to the conduction band (arrow 3), or from the valence band to Bi^{3+} (arrow 4). Free charge carriers are trapped to form Bi^{4+} or Bi^{2+} (arrows 1 and 2). This is the so-called charging or storage phase. By thermal or photon stimulation, trapped charge carriers are released again, transported through the CB or the VB to eventually generate Bi^{3+} A-band recombination lumines-

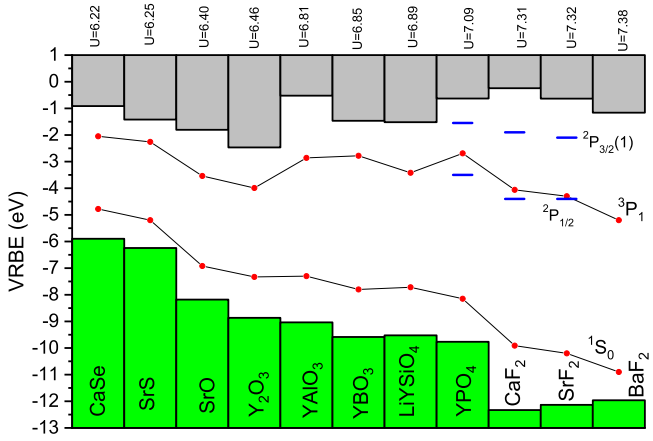

Fig. 4. Stacked VRBE diagram of a selection of compounds organized with increasing U-value with the Bi^{3+} ground and excited state location. For three compounds, the Bi^{2+} ground and excited states are also shown. The used data are from [20].

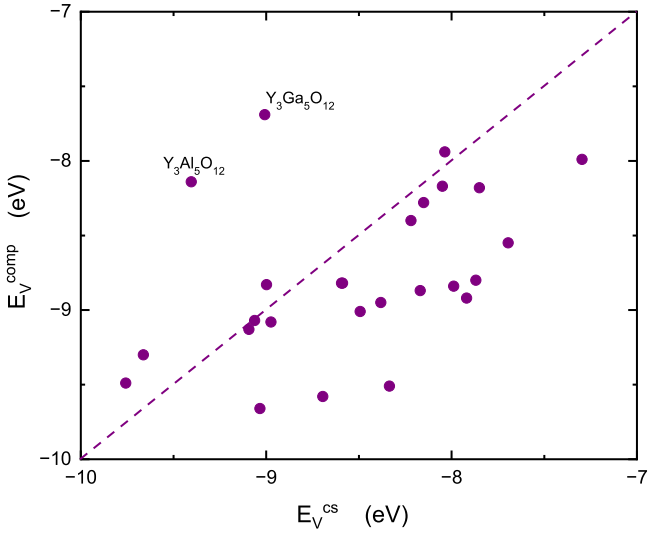

Fig. 5. The energy E_V^{comp} at the top of the valence band as computed with the vacuum and slab method against E_V^{cs} as derived with the semi-empirical chemical shift method.

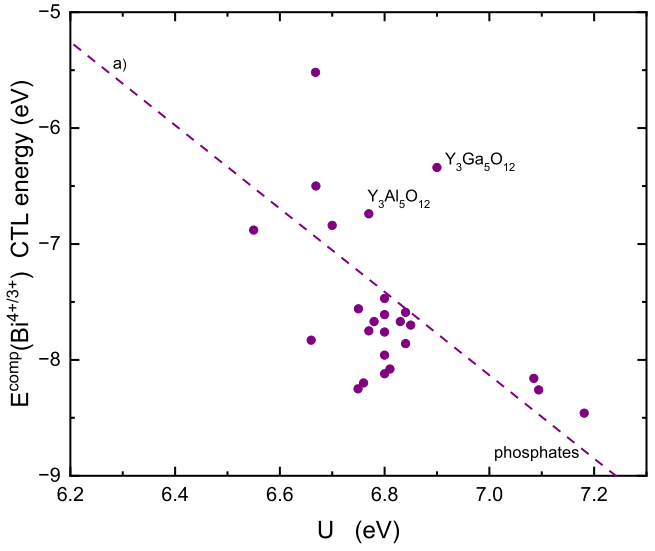

Fig. 6. The computed $E^{comp}(Bi^{4+/3+})$ CTL energies obtained when computed Bi^{3+}→CB MMCT energies are subtracted from computed CB-bottom energies E_C^{comp}. Energies are displayed against the U-value of the compound. Dashed line a) is the expected trend from Ref. [5].

cence (arrow 5). Fig. 2 also illustrates metal-to-metal charge transfer (MMCT) luminescence (arrow 6). The optical excitation to the CB (arrow 3) and emission from the reversed transition (arrow 6) are known as D-band excitation and D-band or MMCT luminescence. When the $Bi^{3+/2+}$ CTL energy is below the $^3P_1$ excited state of Bi^{3+}, Bi^{3+} A-band emission can be quenched by electron transfer to a nearby Bi^{3+} (see arrow 7). Back transfer of the electron from Bi^{2+} to create the ground state of the parent Bi^{3+} leads to so-called Bi-Bi pair emission and/or quenching of A-band emission (see arrow 8) [19,34].

2. Results and discussion

Knowledge and understanding of Bi CTL energies are important to understand, predict, and engineer all the phenomena dealing with charge carrier transfer. Awater and Dorenbos in 2017 reviewed the energy of Bi^{3+} to conduction band MMCT energies in 117 different compounds [5]. Together with information on the VRBE at the VB-top and

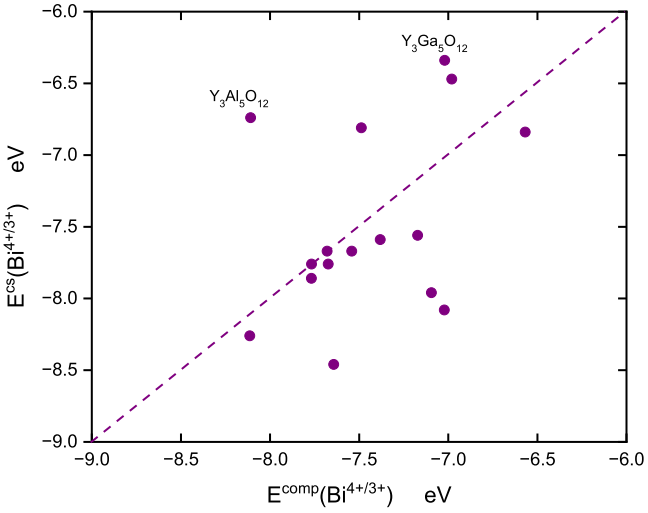

Fig. 7. Comparison of the $Bi^{4+/3+}$ charge transition level energies relative to the vacuum level as obtained with experimental methods ($E^{cs}(Bi^{4+/3+})$) and with computational methods ($E^{comp}(Bi^{4+/3+})$).

CB-bottom, the study provided for the first time the energy of the $Bi^{4+/3+}$ CTLs relative to the vacuum level. Fig. 3 reproduces the results from Awater and Dorenbos. The $Bi^{4+/3+}$ CTL energies are displayed by the data symbols along line a) against the environmental U-value of the compounds. The CTL energy increases from ≈-9 eV in fluorides with U-value between 7.2 and 7.4 eV to ≈-5 eV in sulfides with U-value around 6.2 eV. The data symbols along line b) in Fig. 3 are the VRBE in the $^3P_1$ excited state of Bi^{3+}. They also increase with a smaller value for U. The energy differences between this excited and ground state, or the A-band energy, are the data points along line c). They decrease with a smaller U.

Fig. 4 shows a stacked VRBE diagram of selected compounds organized with increasing U-value. It starts with the highly covalent compounds CaSe and SrS, where the nephelauxetic effect is large and U is small. It ends with the highly ionic alkaline earth fluorides with a small nephelauxetic effect and a large value for U. The Bi^{2+} $^2P_{1/2}$ ground and $^2P_{3/2}(1)$ excited state levels for YPO_4, CaF_2, and SrF_2 are also shown. The same trends with an increase of U are seen as in Fig. 3. Note, that the energy E_V at the valence band top tends to decrease and the band gap tends to widen with the increase of U. The Bi^{2+} ground state falls below the $^3P_1$ excited state of Bi^{3+}. This implies that the A-band luminescence quenching route illustrated by arrow 7) and 8) in Fig. 2 or Bi-Bi pair emission illustrated by arrow 8) becomes probable at high Bi-concentration.

The precision of the CTL energies from Ref. [5] hinges on the precision of the energy at the bottom of the CB and how well the energy of the Bi^{3+}→CB MMCT band represents the energy difference between the $Bi^{4+/3+}$ CTL and the bottom of the CB (see arrow 3 in Fig. 2). The CB-bottom energy relative to the vacuum level was established with the chemical shift model for lanthanide-doped compounds [21,22]. This model provides an empirical expression that relates the $Eu^{3+/2+}$ CTL energy $E(Eu^{3+/2+})$ with the U-value

$$E(Eu^{3+/2+}) = -24.92 + \frac{18.05 - U}{0.777 - 0.0353U}. \quad (1)$$

With U ranging from 7.4 eV to 6.2 eV, the $Eu^{3+/2+}$ CTL energy is remarkably invariant with the type of compound. It always appears near -4 eV. A few 0.1 eV lower for the fluorides and a few 0.1 eV higher for the sulfides and the selenides.

Knowledge of the energy $E^{CT}(Eu^{3+})$ of the VB to Eu^{3+} charge transfer band provides the energy E_V at the VB-top with

$$E_V = E(Eu^{3+/2+}) - E^{CT}(Eu^{3+}). \quad (2)$$

Table 1
A compilation of compounds studied by computational methods in Ref. [24–32] with the computed VRBE energy at the VB-top (E_V^{comp}), the CB-bottom (E_C^{comp}), and the $Bi^{4+/3+}$ CTL energy $E^{comp}(Bi^{4+/3+})$. For the same set of compounds, the U value, the energy E^{CT} of VB→ Eu^{3+} electron transfer, and the energy E^{ex} for host exciton creation are provided. This data then provides E_V^{cs} and E_C^{cs} with the chemical shift method. With Bi^{3+} MMCT energies from [5], the $E^{cs}(Bi^{4+/3+})$ are obtained. Numbers in italics refer to compounds where computations were performed relative to the energy at the VB-top and not the vacuum level. In those cases, E_V^{comp} was set equal to E_V^{cs} to obtain E_C^{comp} and $E(Bi^{4+/3+})$. All energies are in eV.

A	U	E^{CT}	E^{ex}	E_V^{cs}	E_C^{cs}	$E^{cs}(Bi^{4+/3+})$	E_V^{comp}	E_C^{comp}	$E^{comp}(Bi^{4+/3+})$	Ref.
$Cs_2NaInCl_6$	6.55	4.20	5.45	–8.05	–2.36	—	–8.17	–2.27	–6.88	[24]
KCl	6.70	4.23	7.52	–8.15	–0.178	–6.57	–8.28	0.0400	–6.84	[24]
$Cs_2NaLaCl_6$	6.67	3.39	6.53	–7.30	–0.425	—	–7.99	–0.150	–6.50	[24]
Cs_2NaYCl_6	6.67	4.13	7.05	–8.04	–0.588	—	–7.94	–0.0100	–5.52	[24]
$LaPO_4$	7.18	4.84	7.95	–9.00	–0.543	–7.64	–8.83	–0.220	–8.46	[25]
YPO_4	7.09	5.55	8.30	–9.66	–0.813	–8.11	–9.30	–0.470	–8.26	[25]
$LuPO_4$	7.08	5.65	8.55	–9.76	–0.625	–	–9.49	–0.520	–8.16	[25]
$LiYGeO_4$	6.94	5.17	6.25	–9.20	–2.64	–	*–9.20*	*–2.36*	*–7.05*	[26]
$LiLuGeO_4$	6.95	5.21	6.25	–9.25	–2.69	–	*–9.25*	*–2.58*	*–7.02*	[26]
$LiScGeO_4$	6.90	5.56	6.40	–9.58	–2.85	–	*–9.58*	*–2.55*	*–7.14*	[26]
$CaSnO_3$	6.80	4.37	4.73	–8.33	–3.43	–	–9.51	–4.66	–8.12	[27]
$LaAlO_3$	6.76	3.90	5.95	–7.85	–1.62	–	–8.18	–2.63	≈ –8.2	[28]
$GdAlO_3$	6.75	4.75	7.30	–8.69	–0.968	–	–9.58	–1.85	–8.25	[28]
$Y_3Al_5O_{12}$	6.77	5.45	6.85	–9.40	–2.18	–8.11	–8.14	–1.79	–6.74	[29]
$YAlO_3$	6.81	5.06	8.00	–9.03	–0.522	–7.02	–9.66	–1.45	–8.08	[28]
$LaGaO_3$	6.80	4.20	5.96	–8.17	–1.92	–7.09	–8.87	–3.18	–7.96	[28]
$Y_3Ga_5O_{12}$	6.90	4.99	6.00	–9.01	–2.72	–7.02	–7.69	–2.34	–6.34	[29]
$LaInO_3$	6.80	4.25	4.95	–8.22	–3.07	–	–8.40	–3.80	–7.47	[28]
$GdVO_4$	6.84	4.00	3.88	–7.99	–3.99	–7.77	–8.84	–3.98	–7.86	[30]
YVO_4	6.80	3.90	3.80	–7.87	–3.95	–7.67	–8.80	–3.94	–7.76	[30]
$LuVO_4$	6.80	3.95	3.74	–7.92	–4.07	–7.77	–8.92	–4.10	–7.76	[30]
$GdNbO_4$	6.83	4.61	4.90	–8.59	–3.50	–7.54	–8.82	–3.60	–7.67	[30]
$YNbO_4$	6.84	4.60	4.96	–8.59	–3.43	–7.38	–8.82	–3.59	–7.59	[30]
$LuNbO_4$	6.85	4.50	4.77	–8.49	–3.54	–	–9.01	–3.74	–7.70	[30]
$GdTaO_4$	6.77	5.02	5.85	–8.97	–2.85	–	–9.08	–3.02	–7.75	[30]
$YTaO_4$	6.78	5.10	6.05	–9.06	–2.72	–7.68	–9.07	–2.98	–7.67	[30]
$LuTaO_4$	6.80	5.12	5.83	–9.09	–2.99	–	–9.13	–2.95	–7.61	[30]
$CaTiO_3$	6.75	3.75	3.76	–7.69	–3.82	–7.17	–8.55	–4.83	–7.56	[27]
$CaZrO_3$	6.66	4.48	5.95	–8.38	–2.15	–	–8.95	–3.01	–7.83	[27]
Gd_2O_3	6.60	4.86	5.35	–8.73	–3.15	–	*–8.73*	*–2.57*	*–6.63*	[31]
Y_2O_3	6.60	5.05	5.87	–8.92	–2.78	–7.49	*–8.92*	*–2.53*	*–6.81*	[31]
Lu_2O_3	6.60	5.10	5.75	–8.97	–2.96	–	*–8.97*	*–2.76*	*–6.93*	[31]
Sc_2O_3	6.60	4.96	6.15	–8.83	–2.38	-6.98	*–8.83*	*–2.34*	*–6.47*	[31]
CaZnOS	6.35	3.80	4.31	–7.56	–3.10	–	*–7.55*	*–2.76*	*–7.07*	[32]

By adding the exciton creation energy E^{ex} and the electron-hole binding energy of that exciton, the energy E_C of free electrons at the CB-bottom is obtained with

$$E_C = E_V + E^{ex} + 0.008 \times (E^{ex})^2. \quad (3)$$

where the electron-hole binding energy is approximated as $0.008 \times (E^{ex})^2$ [23].

Past five years, computational studies have appeared on Bi^{3+} doped inorganic compounds [24–32]. The $Bi^{4+/3+}$ CTL energy above the VB-top was first computed. When this is combined with the VRBE at the VB-top computed by the slab and vacuum method, the $Bi^{4+/3+}$ CTL energy relative to the vacuum level is obtained. This means that we have both the semi-empirical chemical shift method and the full computational method to derive the $Bi^{4+/3+}$ CTL energy relative to the vacuum level. The results from both methods are compiled in Table 1. The values for U, E^{CT}, and E^{ex} provide E_V^{cs} and E_C^{cs} with the chemical shift model using Eqs. (1)–(3). E^{CT} and E^{ex} are slightly temperature dependent, and we used the (estimated) values that pertain to room temperature [33]. With the Bi^{3+}→VB MMCT energies from Awater and Dorenbos [5], the $E^{cs}(Bi^{4+/3+})$ CTL energies are obtained for 16 different compounds in Table 1. The E_V^{comp} and E_C^{comp} are energies from the computational studies. Adding the computed $Bi^{4+/3+}$ CTL energy difference with the VB-top to E_V^{comp}, the $Bi^{4+/3+}$ CTL energy $E^{comp}(Bi^{4+/3+})$ relative to the vacuum level is obtained. For the Li(Y,Lu,Sc)GeO_4, the $(Gd,Y,Lu,Sc)_2O_3$, and CaZnOS, the published energies were computed relative to the VB-top [26,31,32]. In those cases we used the E_V^{cs} values to obtain E_V^{comp} and the $E(Bi^{4+/3+})$ CTL energies. Those data are in italic font in Table 1.

Fig. 5 shows the energy E_V^{comp} at the VB-top computed with the slab and vacuum method against the energy E_V^{cs} derived with the chemical shift method and experimental data from lanthanide spectroscopy. The E_V^{comp} for the garnet compounds $Y_3Al_5O_{12}$ (YAG) and $Y_3Ga_5O_{12}$ (YGG) appears ≈1.3 eV higher than E_V^{cs}. There is an abundance of data available on lanthanide spectroscopy and charge carrier trapping in garnet compounds, and assuming a 1.3 eV error in E_V^{cs} would not be consistent. The deviation, therefore, hints towards a systematic error in the computations. All other compounds have similar or less than 1 eV smaller value than E_V^{cs}.

Fig. 6 shows the computed $E^{comp}(Bi^{4+/3+})$ CTL energies against the U-value of the compound. Dashed line a) is the same as solid line a) constructed through the results from Awater and Dorenbos [5] in Fig. 3. The $E^{comp}(Bi^{4+/3+})$ CTL energies tend to follow the same line. Note that the data may scatter 1 eV from the dashed line, but the same applies to the data in Fig. 3. This does not imply that either the computed or the experimental values contain such large errors since there is no reason to believe or to require that data should show smaller deviation from line a). The U-value is an environmental parameter that works well for the lanthanides, but it may work less good for Bi. Furthermore, the U-value may carry ±0.1 eV error. Nevertheless, the results in Figs. 5 and 6 demonstrate that the computational method and the method based on the chemical shift model provide consistent trends and reasonable

quantitative agreement. In that sense both approaches complement and justify each other.

In Fig. 7, the experimentally derived $E^{cs}(Bi^{4+/3+})$ CTL energies for the 16 compounds in Table 1 are compared with the computational $E^{comp}(Bi^{4+/3+})$ CTL energies. Clear correlations are again observed with the garnet $Y_3Al_5O_{12}$ as the largest outlier data point.

In summary, charge carrier trapping by or charge carrier release from Bi^{4+}, Bi^{3+}, or Bi^{2+} is related to the energy of the charge transition levels of $Bi^{4+/3+}$ and $Bi^{3+/2+}$ relative to VB or CB of the compound. In 2017, the chemical shift method was applied to derive those CTL energies relative to the vacuum level. In the past five years, computational studies have appeared to derive the same. In this work, the results of both methods have been compared. They provide consistent results. The trends with the type of compound are the same, and usually the obtained CTL energies agree within ±0.5 eV. Larger deviations do occur, which then may hint towards either experimental or computational errors.

Declaration of competing interest

The authors declare that they have no known competing financial interests or personal relationships that could have appeared to influence the work reported in this paper.

Data availability

All data used is in Table 1 of the manuscript and references where data were obtained are provided in the manuscript.

References

[1] P. Dorenbos, J. Mater. Chem. C. 11 (2023) 8129.
[2] A. Ranfagni, D. Mugnai, M. Bacci, G. Viliani, M.P. Fontana, Adv. Phys. 32 (1983) 823.
[3] L. Wang, Q. Sun, Q. Liu, J. Shi, J. Solid State Chem. 191 (2012) 142.
[4] M. Amer, P. Boutinaud, Phys. Chem. Chem. Phys. 19 (2017) 2591.
[5] R.H.P. Awater, P. Dorenbos, J. Lumin. 184 (2017) 221.
[6] P. Dorenbos, J. Lumin. 267 (2024) 120358.
[7] P. Boutinaud, Phys. Chem. Chem. Phys. 25 (2023) 11027.
[8] F.A. Kröger, J. Th, G. Overbeek, J. Goorlissen, J.V.D. Boomgaard, Electrochem. Soc. 96 (1949) 132.
[9] G. Blasse, A. Bril, The J. Chem. Phys. 48 (1968) 217.
[10] M.A. Hamstra, H.F. Folkerts, G. Blasse, J. Mater. Chem. 4 (1994) 1349.
[11] H.-T. Sun, J. Zhou, J. Qiu, Prog. Mater. Sci. 64 (2014) 1.
[12] R. Cao, Y. Cao, T. Fu, S. Jiang, W. Li, Z. Luo, J. Fu, J. Alloys Compd. 661 (2016) 77.
[13] G. Boulon, J. Phys. Paris (1971) 333.
[14] H.C. Swart, R.E. Kroon, Opt. Mater. X 2 (2019) 100025.
[15] Y. Tang, M. Deng, M. Wang, X. Liu, Z. Zhou, J. Wang, Q. Liu, Adv. Opt. Mater. 2022, p. 2201827.
[16] W. Fang, W. Shangguan, Int. J. Hydrog. Energy 44 (2019) 895.
[17] X. Meng, Z. Zhang, J. Mol. Catal. A Chem. 423 (2016) 533.
[18] P. Boutinaud, Inorg. Chem. 52 (2013) 602 .
[19] P. Boutinaud, J. Lumin. 197 (2018) 228.
[20] P. Dorenbos, ECS J. Solid State Sci. Technol. 10 (2021) 086002.
[21] P. Dorenbos, Phys. Rev. B 85 (2012) 165107.
[22] P. Dorenbos, Phys. Rev. B 87 (2013) 035118.
[23] P. Dorenbos, Opt. Mater. 69 (2017).
[24] M. Liu, C.-K. Duan, P.A. Tanner, C.-G. Ma, M. Yin, J. Phys. Chem. C 125 (2021) 26670.
[25] Z. Feng, B. Lou, M. Yin, H.-T. Y.-Y. Yeung, C.-K. Sun, Duan, Inorg. Chem. 60 (2021) 4434.
[26] Z. Qiao, X. Wang, C. Heng, W. Jin, L. Ning, Inorg. Chem. 60 (2021) 16604.
[27] B. Lou, J. Wen, J. Cai, M.Y.-Y. Yeun, C.-K. Yin, Duan, Phys. Rev. B 103 (2021) 075109.
[28] B. Lou, J. Wen, L. Ning, M. Yin, C.-G. Ma, C.-K. Duan, Phys. Rev. B 104 (2021) 115101.
[29] B. Jiang, Q. Liu, F. Chi, B. Lou, Materials 18 (2025) 5082.
[30] Z. Feng, B. Lou, Q. Chen, M. Yin, C.-G. Ma, C.-K. Duan, Inorg. Chem. 60 (2021) 16614.
[31] H. Bai, B. Lou, M.S. Kurboniyon, A. Suchocki, M.G. Brik, J. Wang, C. Ma, Materials 17 (2024) 2039.
[32] Q. Kougong, B. Lou, M.G. Brik, Materials 18 (2025) 657.
[33] P. Dorenbos, J. Lumin. 269 (2024) 120443.
[34] H.P. Roy, P. Awater, Dorenbos, J. Lumin. 188 (2017) 487.